

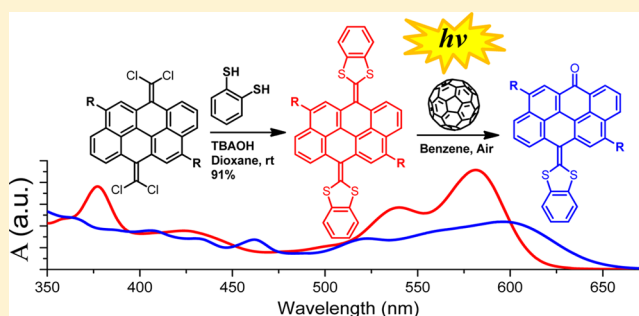
# Superextended Tetrathiafulvalene: Synthesis, Optoelectronic Properties, Fullerenes Complexation, and Photooxidation Study

Jean-Benoît Giguère and Jean-François Morin\*

Département de Chimie and Centre de Recherche sur les Matériaux Avancés (CERMA), Université Laval, 1045 Avenue de la Médecine, Québec City, Québec G1V 0A6, Canada

**S** Supporting Information

**ABSTRACT:** Superextended tetrathiafulvalene compounds were prepared by the substitution of *gem*-dichlorovinylene with 1,2-benzenedithiol. This strategy allowed for the efficient synthesis of a highly  $\pi$ -extended 9,10-bis(benzo-1,3-dithiol-2-ylidene)-9,10-dihydroanthracene (sExTTF) moiety, which exhibits an intense light absorption in the visible spectrum and a reversible oxidation process. A macrocyclic host for fullerenes containing two sExTTF units was synthesized. Complexation studies revealed that fullerenes promote the photooxidation of the 1,3-dithiolylidene bond. This grants new insights into the nature of the low-energy band that appeared in several reports on fullerene complexation with hosts containing the 1,3-dithiolylidene moiety.



## INTRODUCTION

The fruitful history of tetrathiafulvalene (TTF) started when Wudl<sup>1</sup> first described its synthesis and properties in 1970. TTF rapidly became the “go-to” organic strong electron donor.<sup>2</sup> It was quickly discovered that charge transfer complexes are formed when it is mixed with electron acceptors. This property opened up a new field of research for synthetic metals,<sup>2</sup> ultimately leading to the discovery of tetrachalcogenofulvalene organic superconductors.<sup>3</sup>

Although excitement about synthetic metals has faded and research efforts have shifted from organic conductors to semiconductors, the 1,3-dithiol-2-ylidene motif (Figure 1) is still of high interest as synthetic efforts have evolved from charge transfer complexes to large  $\pi$ -extended structures.<sup>2,4</sup> The 1,3-dithiol-2-ylidene moiety is a versatile electron-donating building block for the design and synthesis of a variety of organic materials. It is often combined with electron acceptors to obtain low-band-gap materials, which allows a precise control of the HOMO–LUMO frontier orbitals.<sup>4a,5</sup> The versatile structural, redox, optical, and electronic properties of TTF-derived compounds led to a range of applications spanning from organic and molecular electronics to supramolecular chemistry.<sup>2,4,6</sup>

Recently, the anthraquinone-derived 9,10-bis(1,3-dithiol-2-ylidene)-9,10-dihydroanthracene moiety (herein abbreviated to exTTF for  $\pi$ -extended TTF, Figure 1) has been the most widely studied TTF-based structure, because it possesses a curved conformation and unique redox properties.<sup>6a,7</sup> These features permit the preparation of highly efficient hosts for fullerenes and carbon nanotubes through a combination of

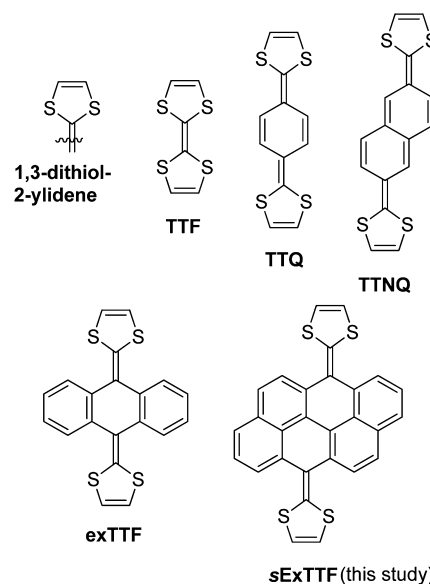


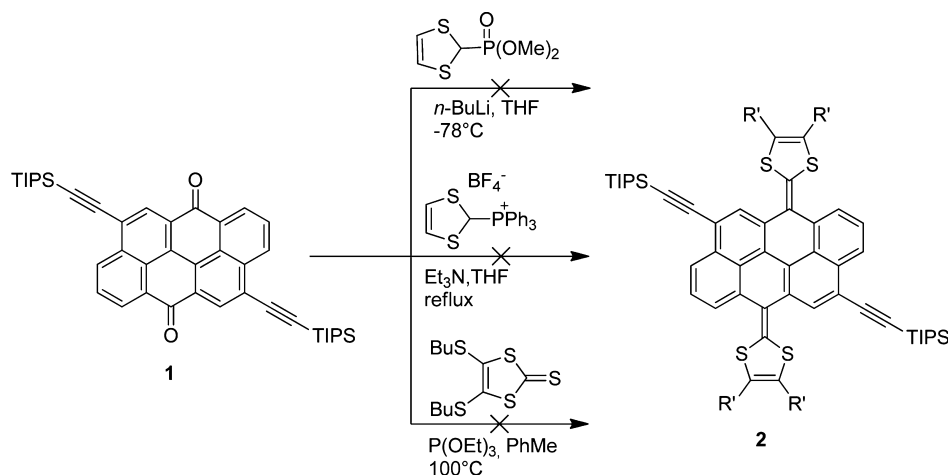
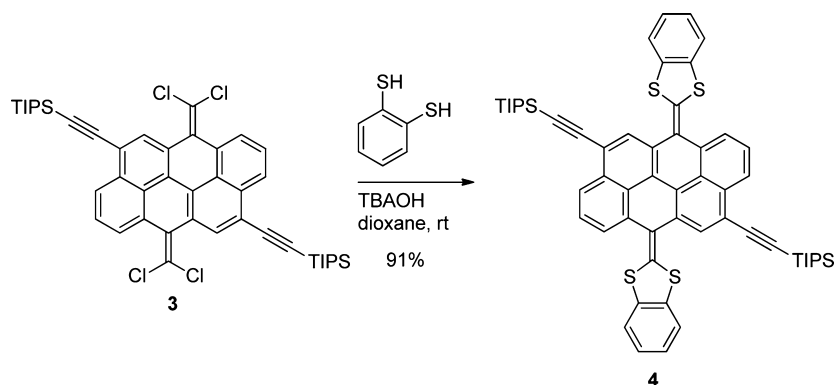
Figure 1. TTF and 1,3-dithiol-2-ylidene extended structures.

concave–convex geometrical matching and electronic complementarity, leading to strong charge transfer interactions.<sup>6a,8</sup>

In 2012, we started to exploit a vat dye, 4,10-dibromoanthanthrone, as a versatile polycyclic aromatic building block for  $\pi$ -extended structures.<sup>9</sup> Initially, we sought to use the anthanthrone motif to prepare the 9,10-bis(1,3-

Received: April 24, 2015

Published: June 12, 2015

Scheme 1. Olefination Route toward the *s*ExTTF ScaffoldScheme 2. Optimized Synthesis of *s*ExTTF 4

dithiol-2-ylidene)-9,10-dihydroanthanthrene motif (abbreviated as *s*ExTTF for *super- $\pi$* -extended TTF, Figure 1) and exploit its highly conjugated polycyclic aromatic structure as a donor component for supramolecular hosts for fullerenes. Until recently, synthetic hurdles have prevented us from achieving this goal, but we have progressed in understanding the reactivities, optoelectronics, and charge transport properties of anthanthrone and anthanthrene structures.<sup>10</sup>

*s*ExTTF offers one of the most  $\pi$ -conjugated TTF-derived structures with two axes of conjugation, the 6,12-quinoidal TTF axis and the 4,10-axis, which offers a second conjugation pathway to the cross-conjugated dithiolylydene moiety. A noteworthy example of an atypical highly conjugated structure is a porphyrin fused with 1,3-dithiol-2-ylidene moieties reported by Sessler et al.<sup>11</sup> Preparation of quinoidal TTF (Figure 1) derivatives such as tetrathioquinodimethane (TTQ)<sup>12</sup> and tetrathionaphthoquinodimethane (TTNQ)<sup>13</sup> has been attempted, but only their iodide complexes were isolated, and the neutral TTQ was reported to be highly air-sensitive.<sup>12</sup> As in the case of the acene-fused exTTF, the polycyclic structure of *s*ExTTF should offer improved stabilization and properties of interest in material sciences such as a lower band gap and increased intermolecular interactions, which should lead to improved electronic coupling and stronger supramolecular interactions.<sup>14</sup>

Herein, we report a mild and improved synthesis of the benzo-1,3-dithiol-2-ylidene moiety from *gem*-dichlorovinylene, leading to the *s*ExTTF scaffold. This synthetic strategy was used to prepare a macrocyclic compound containing two *s*ExTTF

units acting as a host for fullerene complexation. Study of the optical and redox properties of the fullerene complexation led to the significant observation of C<sub>60</sub>-sensitized photooxidation of the 1,3-dithiol-2-ylidene moiety.<sup>15</sup> This finding brings new insights into the nature of the low-energy band that has appeared in several reports when fullerenes interact with hosts containing the 1,3-dithiol-2-ylidene moiety.

## RESULTS AND DISCUSSION

**Synthesis.** Although the syntheses of TTF derivatives are well-known,<sup>4a,5b,16</sup> it proved rather challenging to prepare the *s*ExTTF scaffold. As shown in Scheme 1, we tried three unsuccessful reactions: (1) Starting from TIPS-appended anthanthrone **1**, the obvious pathway to form a dithiolylydene bond was the Wittig–Horner olefination with 1,3-dithiol phosphonate<sup>17</sup> (Scheme 1). To our surprise, and as we previously reported in the case of organolithium compounds,<sup>9</sup> this led to the formation of the ketyl radical anion, precluding any nucleophilic attack on the carbonyl. (2) Wittig olefination with the less nucleophilic triphenylphosphonium reagent left the anthanthrone scaffold intact. (3) The triethylphosphite-mediated olefination using 4,5-bis(butylthio)-1,3-dithiol-2-thione<sup>18</sup> led to the decomposition of the starting material.

Since the direct olefination approach from the anthanthrone's finicky carbonyls proved unsuccessful, we turned our efforts to a postolefination functionalization approach inspired by a recent report on S-vinylation of vinyl halides.<sup>19</sup> Our efforts are shown in Scheme 2.

In 1926, Hurtey and Smiles<sup>20</sup> used a strategy involving substitution of tetrachloroethylene with 1,2-benzenedithiol to synthesize the first tetrathiafulvalene derivative. This approach was later studied in greater detail for the synthesis of benzo-TTF derivatives.<sup>21</sup> Although the published yields were generally low, we used these conditions as a starting point. A major breakthrough came with the stoichiometric use of soluble tetrabutylammonium hydroxide ((TBA)OH), instead of alkali-metal bases, to deprotonate the commercially available 1,2-benzenedithiol to form a soluble bithiophenolate reactant.

This simple modification led to a dramatic improvement of the yield and reaction time, and we achieved complete conversion at room temperature. The high reactivity of *gem*-dichlorovinylene toward substitution may be attributed to the stabilization by delocalization of the carbanion formed upon nucleophilic attack by the thiolate, similarly to what is observed in the case of a nucleophilic aromatic substitution-type mechanism ( $S_NAr$ ).<sup>21c</sup> Hence, we obtained an excellent yield (91%) of TIPS-*s*ExTTF **4** under mild conditions. This improved methodology should also apply to complex structures and asymmetric substrates.

**DFT Calculations.** The frontier orbitals of *s*ExTTF **4** were calculated at the B3LYP/6-31G\*\* level of theory.<sup>22</sup> Figure 2

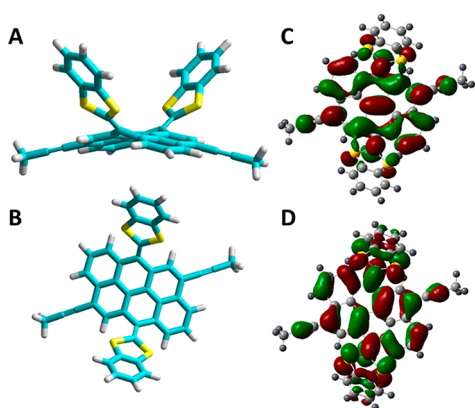


**Figure 2.** DFT-optimized structure for *s*ExTTF **4**: (A) side view, (B) top view. Frontier orbitals from the top view: (C) LUMO, (D) HOMO.

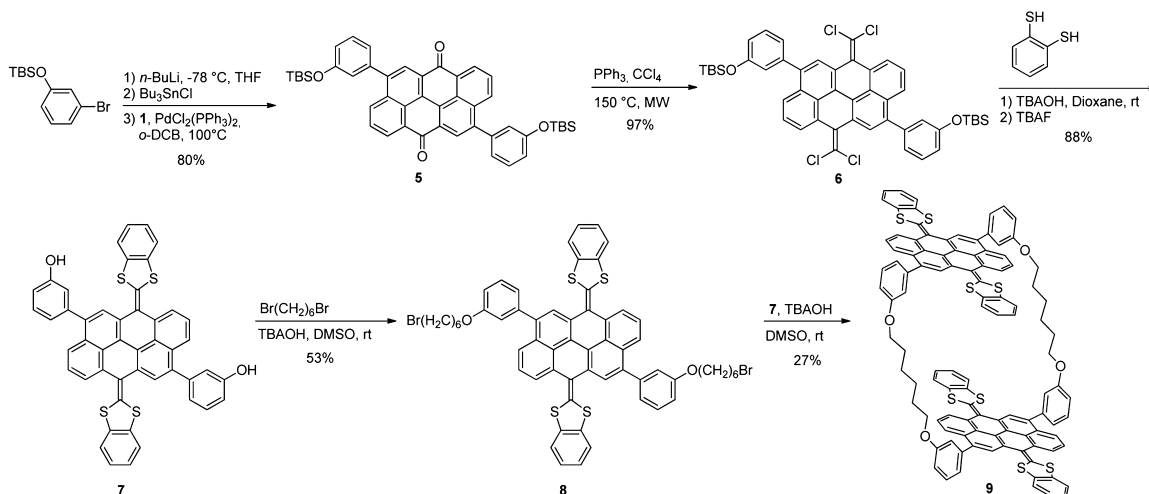
shows the optimized structure alongside the HOMO–LUMO distribution. The *s*ExTTF scaffold adopts a *syn*-folded saddle-shaped configuration with a dihedral angle between the two aromatic naphthalene planes of 28° (38° for exTTF from the crystal structure<sup>23</sup>) and a 38° angle between the 1,3-dithiol-2-ylidene bond and the C(6)–C(10) vector, which is almost identical to that of exTTF. Relief of the steric strain between the large sulfur atoms and the *peri*-hydrogens results in a bent structure that is slightly less curved than that of exTTF, reasonably attributed to the rigidity of the polycyclic core.

According to our calculations, the HOMO is distributed over the whole molecule, while the LUMO does not populate the dithiobenzene ring. Unfortunately, only fiberlike crystals were grown, and they proved unsuitable for X-ray diffraction to confirm the saddle-shaped configuration.

The curved structure should offer extensive  $\pi$ -contact with fullerenes, as for exTTF. To assess the potential of the *s*ExTTF scaffold in supramolecular chemistry, we designed macrocyclic host **9** as an analogue of Aida's cyclic porphyrin hosts.<sup>24</sup> Interestingly, *s*ExTTF **4** and the porphyrin scaffolds have very similar structural parameters with a C(4)–C(12) distance of 7.01 Å for **4** compared with a C(*meso*)–C(*meso*) distance of 7.12 Å for the porphyrin scaffold (Figure S1, Supporting Information).<sup>25</sup>

Scheme 3 describes the straightforward synthesis of host **9**. Anthanthrone **5** was synthesized using Stille coupling from in situ prepared a 3-(tributylstannyl)phenoxy compound and vat dye 4,10-dibromoanthanthrone. The phenolic groups were protected with TBS to induce good solubility and ensure compatibility with the Ramirez olefination step. Then a highly efficient bis(*gem*-dichloro)olefination under microwave-assisted conditions<sup>9</sup> was performed and cleanly yielded compound **6**. Substitution of the *gem*-dichloroylidene **6** with 1,2-benzenedithiol under the conditions described above caused partial cleavage of the TBS protecting groups. Addition of excess TBAF allowed the recovery of bisphenol **7**. We used a two-step alkylation process to simplify the purification process and improve the macrocyclization yield. Also, the use of a soluble tetrabutylammonium hydroxide base ensured the solubility of all species at room temperature. Thus, alkylation of **7** with excess 1,6-dibromohexanes yielded bisalkylated **8**, which was further macrocyclized with compound **7** to yield host **9** with an acceptable yield.

### Scheme 3. Synthesis of Bis-*s*ExTTF Macrocyclic Host **9**



**Fullerene Complexation and Photooxidation.** The extended electron-rich polycyclic curved structure of host **9** should offer strong interactions with fullerenes. Moreover, its structure resembles that of previously reported “strapped porphyrins”, which efficiently bind fullerenes.<sup>26</sup> For reasons explained in the next section, argon-purged solvents were used for the complexation experiments to limit photooxidation (*vide infra*). UV–vis titration experiments from toluene (good solvent) and a toluene/acetonitrile (2:1) solvent mixture (increased polarity and decreased fullerene solubility) were performed to quantify the host’s affinity for fullerenes  $C_{60}$  and  $C_{70}$ . The results are summarized in Table 1.

**Table 1. Summary of the Binding Constants between Host 9 and Fullerenes**

solvent <sup>a</sup>	$K_a(C_{60})^b$ ( $M^{-1}$ )	$K_a(C_{70})^b$ ( $M^{-1}$ )	$K_a(C_{70})/K_a(C_{60})$
PhMe	12000		
PhMe/ACN (2:1)	43000	260000	6.0

<sup>a</sup>PhMe = toluene, and ACN = acetonitrile. <sup>b</sup>UV–vis (298 K). The  $K_a$  values were calculated by the nonlinear least-squares method,<sup>27</sup> and the value reported is the average of the  $K_a$  measured with  $\Delta A$  at 420 and 546 nm.

In all titration experiments, the fullerene absorption was experimentally subtracted to isolate the host absorption and simplify the analysis. The complexation between fullerenes  $C_{60}$  and  $C_{70}$  with host **9** was studied using UV–vis spectroscopy by monitoring the 420 and 546 nm bands upon addition of a fullerene solution. Figure 3 shows a representative UV–vis spectrum of a complexation experiment.

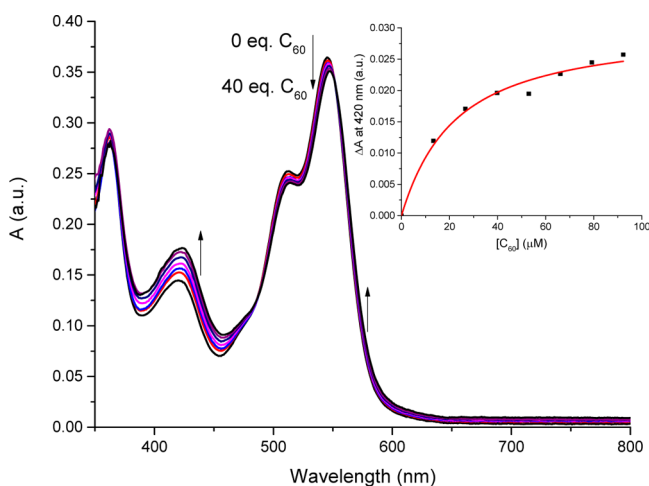


**Figure 3.** UV–vis titration experiment of host **9** ( $3.9 \mu M$ ) in toluene upon addition of  $C_{60}$ . Inset: absorbance difference at 420 nm.

Host **9** has a broad absorption spectrum with a  $\lambda_{max}$  at 550 nm. The addition of  $C_{60}$  leads to the formation of a supramolecular complex with a calculated association constant ( $K_a$ ) of  $12000 M^{-1}$  in toluene.

Although two isosbestic points are present at 370 and 552 nm, the extent of the spectral changes is limited relative to the spectra of the reported exTTF-type hosts, which exhibit the appearance of a strong band at 475 nm.<sup>7c,28</sup> Inclusion of  $C_{60}$  increases absorbance in the 370–480 nm region and weakens it in the 487–552 nm region with a limited bathochromic shift of 2 nm. This characteristic resembles porphyrin-type hosts more

than exTTF hosts.<sup>24b</sup> Addition of acetonitrile as a marginal solvent for fullerenes increases the  $K_a$  value to  $43000 M^{-1}$  for  $C_{60}$  and  $260000 M^{-1}$  for larger  $C_{70}$  (Figures S2 and S3, Supporting Information).

The selectivity factor ( $K_a(C_{70})/K_a(C_{60})$ ) of 6.0 for  $C_{70}$  is quite high, as is expected from the egg-shaped and flatter structure that should allow for improved interactions with the large polycyclic core. A reliable Job plot could not be obtained because of the minimal spectral difference between the free and complexed host. Nevertheless, a 1:1 complex is expected because of its structure being very similar to those of the reported cyclic hosts.<sup>24,26</sup> Although a structure–property analysis of the structural and electronic effects is difficult without a direct reference point, a close match would be Aida’s macrocyclic *meso* and  $\beta$ -unsubstituted zinc porphyrin dimer with an association constant of  $100000 M^{-1}$  measured in a 1:1 toluene/THF mixture. Their affinity for fullerenes is of the same order of magnitude, which is indicative of sExTTF’s potential in the supramolecular chemistry of carbon nanostructures.

During our preliminary experiments without deliberate oxygen degassing, we observed that the intensity of the host **9**– $C_{60}$  band ascribed to the charge transfer at 600 nm appeared to be dependent on the light irradiation conditions. A more intense, red-shifted charge transfer band was observed when the samples were left under ambient light conditions, even for a short period.

We initially speculated that this might be an exciting light-induced complexation event, which prompted us to investigate further. As a control study, we irradiated a sample of host **9** ( $5 \mu M$ ) and  $C_{60}$  ( $20 \mu M$ ) with a 500 W halogen lamp and measured the absorption spectrum (Figure 4). This light

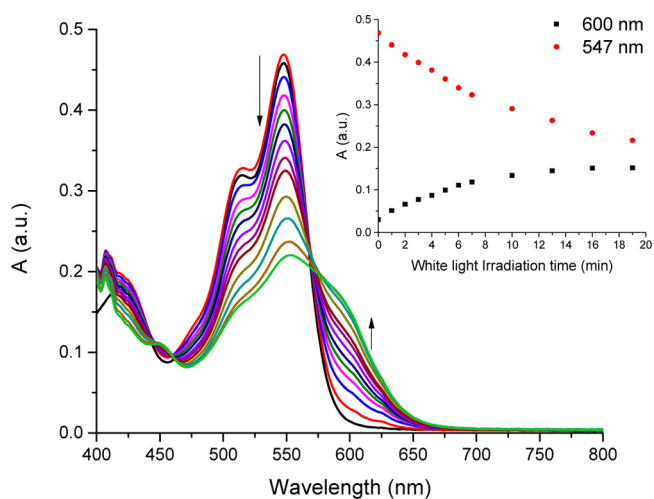
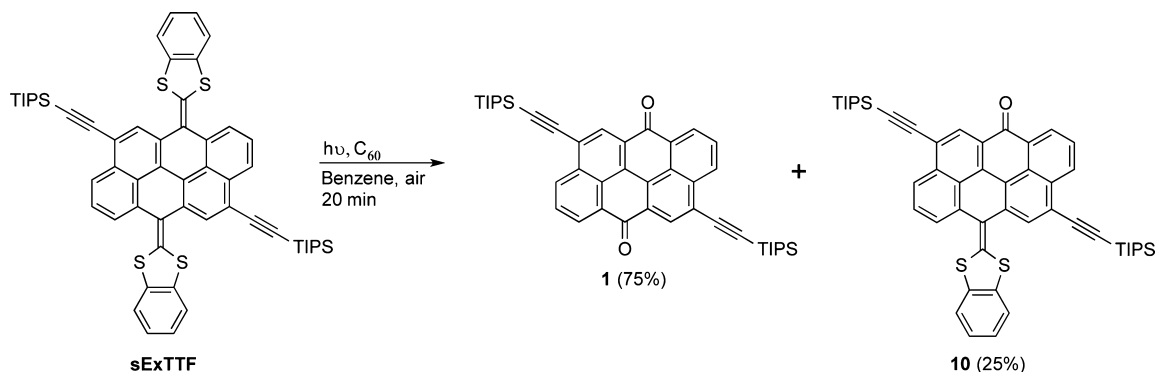


**Figure 4.** Absorption spectra of a mixture of **9** ( $5 \mu M$ ) and  $C_{60}$  ( $20 \mu M$ ), absorption subtracted from spectra) in chlorobenzene with different irradiation times with the absorbance at 600 nm (black markers) and 547 nm (red markers) plotted against the irradiation time in the inset.

“titration” experiment resulted in a spectral signature very similar to that obtained when fullerene is added to exTTF-based hosts.<sup>7a,c,28</sup> A diminution of the 547 nm absorption band with an increase of the “charge transfer” band at 600 nm was observed with a clear isosbestic point at 570 nm.

The absorption against irradiation time is plotted in the Figure 4 inset and follows an exponential decay function, as also

## Scheme 4. Preparative Fullerene-Sensitized Photooxidation Reaction



reported by Zhao for  $\pi$ -conjugated oligomers.<sup>15</sup> Further control experiments indicated that host **9** was photostable under white light without the presence of  $\text{C}_{60}$  (Figure S4, Supporting Information). Furthermore, no spectral change occurred when the solutions were kept in the dark at either room temperature or 90 °C (Figure S5, Supporting Information).

To uncover the precise species at play, we performed NMR analysis of a mixture of **8** (as a more soluble and simple spectrum surrogate for host **9**) and  $\text{C}_{60}$  before and after irradiation (Figure S6, Supporting Information). In the aromatic region, new sharp downfield-shifted peaks arose, which are indicative of a new species that is not attributed to light-induced supramolecular interactions.

To shed light on this unforeseen reaction, we performed a preparative photochemistry experiment where a mixture of compound **4** and  $\text{C}_{60}$  (0.5 equiv) was irradiated in aerated benzene. After 20 min, the conversion of **4** was complete with a clean conversion to two compounds that were isolated in high yield (Scheme 4).<sup>29</sup>

<sup>1</sup>H NMR and HRMS allowed the determination of two oxidation products: anthanthrone **1** and push-pull compound **10**. Fullerenes such as  $\text{C}_{60}$  are well-known singlet oxygen sensitizers via triplet energy transfer, and are used in photodynamic therapy.<sup>30</sup> Fullerenes have also been used to photocatalyze the oxidation of alkenes.<sup>31</sup> The proposed mechanism follows a [2 + 2] cycloaddition with <sup>1</sup>O<sub>2</sub> at the electron-rich 1,3-dithiol-2-ylidene bond to a 1,2-dioxetane-type intermediate, which readily decomposes to the corresponding ketones.<sup>15,32</sup>

Interestingly, the ethynylene bond remains intact under the conditions used, asserting the dithiolylydene bond sensitivity toward oxidation as it occurs even under mild ambient conditions during the course of UV-vis titration experiments. It is worth pointing out that the oxidized product of host **9** was observed in the MALDI-TOF spectrum when mixed with  $\text{C}_{60}$  (Figure S8, Supporting Information). Fullerene sensitization via electron and/or energy transfer from the highly absorbing sExTTF unit could explain this efficient process, although further photophysical studies are needed to prove the mechanism.

To ensure that the photooxidation reaction was not specific to sExTTF, a benzo-exTTF<sup>33</sup>/ $\text{C}_{60}$  sample was irradiated, and the same spectroscopic evidence was observed (Figure S7, Supporting Information), indicating that special precautions should be taken when performing optical measurements on oxidation-sensitive double bonds containing substrates mixed with fullerenes.<sup>15</sup>

**Optical and Electrochemical Properties.** The absorbance spectra of compounds **4** and **10** are presented in Figure 5.

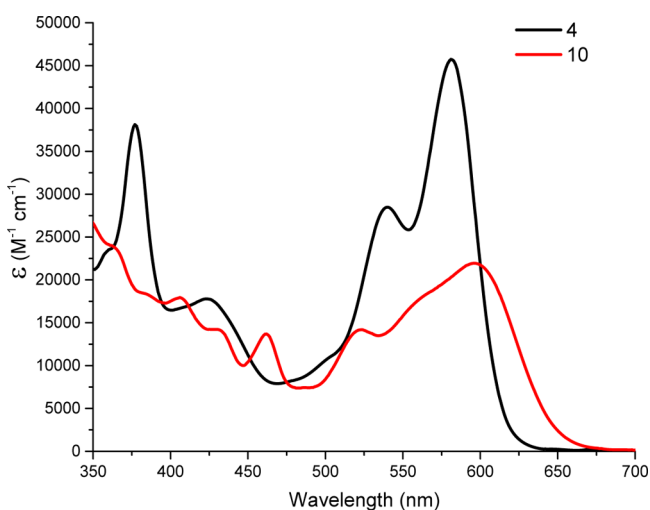


**Figure 5.** UV-vis spectra of compounds **4** and **10** at ca. 15  $\mu\text{M}$  in toluene.

TIPS-appended sExTTF **4** presents a broad absorption spectrum with a  $\lambda_{\text{max}}$  of 581 nm with a remarkably high extinction coefficient ( $\epsilon$ ) of 45 000  $\text{M}^{-1} \text{cm}^{-1}$ . Oxidation of one 1,3-dithiovinylene bond to the carbonyl in compound **10** causes an 18 nm red shift of the maximum to 597 nm as a result of intramolecular charge transfer (push-pull effect).<sup>14a</sup> The spectral signature of compound **10** corroborates the proposed light-induced degradation pathway for the red-shifted absorbance of host **9** in Figure 4.

The electrochemical properties of selected compounds were analyzed using cyclic voltammetry in dichloromethane with a  $\text{Bu}_4\text{NPF}_6$  electrolyte, two platinum wire electrodes, and a Ag/AgCl reference electrode. The results are reported in Table 2.

**Table 2. Summarized CV Electrochemical Potentials<sup>a</sup>**

compd	$E_{\text{ox}}$ (V)	$E_{\text{red}}$ (V)	compd	$E_{\text{ox}}$ (V)	$E_{\text{red}}$ (V)
<b>4</b>	0.35		<b>9</b> / $\text{C}_{60}$ (1:1)	0.28	-0.51
<b>9</b>	0.24		$\text{C}_{60}$		-0.51
<b>10</b>	0.71	-0.50			

<sup>a</sup>Redox potentials were measured at the onset.  $V$  values vs Ag/AgCl at a scan rate of 100  $\text{mV s}^{-1}$ . For reference, the  $\text{Fc}/\text{Fc}^+$   $E_{1/2}$  was measured at 0.51 V vs Ag/AgCl.

Compound **4** presents a single, reversible, two-electron oxidation process with a potential onset of 350 mV, which is an  $E_{1/2ox}$  about 150 mV lower than that of the parent benzo-exTTF (Figure 6).<sup>33</sup> A large cathodic/anodic peak separation of

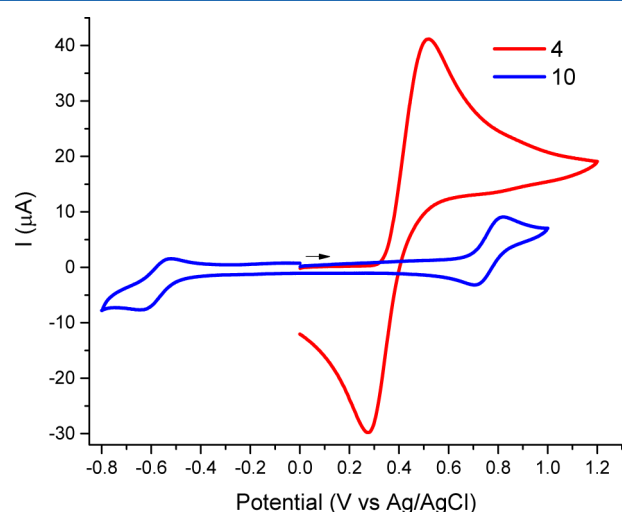


**Figure 6.** Cyclic voltammetry of compounds **4** and **10**.

240 mV is indicative of a large conformation change during the redox process. Although the two-electron oxidation process causes aromatization of the dihydroanthanthrene core, no new aromatic Clar sextets, usually responsible for thermodynamic stabilization of  $\pi$ -conjugated molecules,<sup>34</sup> are formed. Nonetheless, the  $\pi$ -extended structure appears to offer improved stabilization of the oxidized state relative to benzo-exTTF with a lower oxidation potential and reversible redox process.

The lower oxidation potential could result in an improved charge transfer interaction with fullerenes. Partially oxidized compound **10** presents amphoteric redox behavior with an oxidation potential shifted by 360 mV to 710 mV (versus compound **4**) and the typical reversible reduction of anthanthrone's carbonyl at  $-500$  mV (Figure 6). Fullerene complexation can be probed electrochemically, as charge transfer interactions should increase the redox potentials of the complexed species.

Interestingly, addition of  $C_{60}$  to host **9** shifted its oxidation potential slightly (40 mV) to 280 mV (Figure 7). Although small, a similar shift was present in multiple scans and could be indicative of ground-state interactions in the complex.<sup>28a</sup> The  $C_{60}$  first reduction potential remained unchanged at  $-510$  mV, which may be due to the multiple possible redox sites present on the fullerene structure.

**Conclusion.** The novel sExTTF scaffold was synthesized by an improved synthesis involving substitution of *gem*-dichlorovinylene by 1,2-benzenedithiol with a (TBA)OH base. The yields were excellent. This simple, facile, and versatile reaction should offer access to complex TTF-type structures relevant to materials sciences.

To assess the potential of the electron-rich polycyclic building block in supramolecular chemistry, a macrocyclic sExTTF-based host for fullerenes was prepared and exhibited an affinity similar to that of porphyrin-type hosts in a "strapped" configuration. UV-vis titration experiments led to the observation of a  $C_{60}$ -sensitized photooxidation reaction, which can be misinterpreted as the spectroscopic signature of

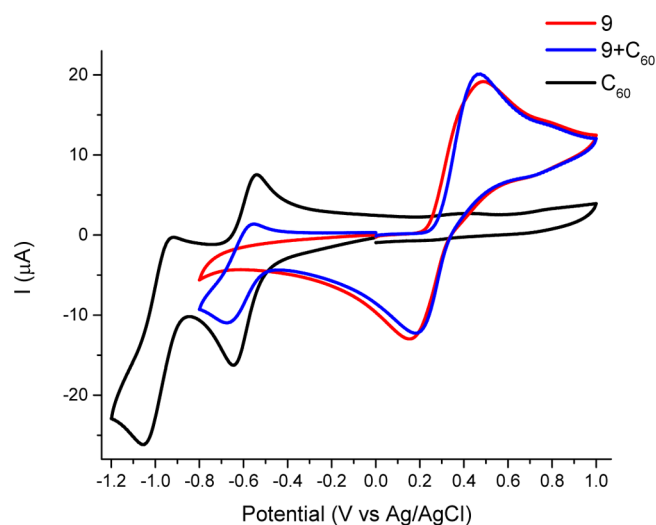


**Figure 7.** Cyclic voltammetry of host **9**,  $C_{60}$ , and a 1:1 mixture of host **9** and  $C_{60}$ .

an intermolecular charge transfer band. This mild oxidation process has strong implications in supramolecular chemistry and materials sciences, as special precautions should be taken when performing complexation experiments with TTF-type molecules.

Fullerene derivatives are the most widely used electron acceptors in organic photovoltaics, and this type of oxidative pathway may cause stability issues. The oxidative sensitivity of electronically rich alkene bonds such as the 1,3-dithiol-2-ylidene motif should be considered when designing new materials.

## EXPERIMENTAL SECTION

**General Methods.** 4,10-Dibromoanthanthrone was provided as a courtesy by Heubach GmbH as product Monolite Red 316801. High-resolution mass spectrometry (HRMS) was performed using a time-of-flight (TOF) LC-MS apparatus equipped with an APPI ion source. MALDI-TOF was performed with a 327 nm laser without the addition of a matrix.

**Optical Measurements.** UV-vis absorption spectra were acquired with a 1 cm path quartz cell equipped with a screw-on Teflon cap.

**Electrochemical Measurements.** All of the cyclic voltammograms were acquired employing a three-electrode potentiostat. The potential was referenced to a Ag/AgCl-saturated KCl electrode, and Pt wires were used as the working and counter electrodes.  $CH_2Cl_2$  with a supporting electrolyte of  $Bu_4NPF_6$  (0.1 M) was sparged using argon for 2 min prior to the electrochemical measurements. For calculation of vacuum levels, the potentials were calibrated against a ferrocene/ferrocenium external standard measured at 0.51 V versus the Ag/AgCl reference electrode.

**Computational Methods.** DFT calculations were carried out with the Gaussian 09 program suite at the B3LYP/6-31G\* level of theory, and the orbital plots are reported at an isovalue of 0.02.

**UV-Vis Titration Experiments.** The titrations were carried out with a solution of host **9** ( $3.9 \mu M$ ) in toluene or in acetonitrile/toluene (2:1; 3 mL) in a quartz cuvette (1 cm path length). A  $C_{60}$  (8 mM) or  $C_{70}$  (1.66 mM) solution in chlorobenzene was added in aliquots (10–50  $\mu L$ ) to the sample cell and reference cell (to experimentally subtract the fullerene absorption). The fitting of the absorbance difference ( $\Delta A$ ) at two wavelengths (420 and 545 nm) against the fullerene concentration was carried out by nonlinear curve fitting with OriginPro 9.0 (OriginLab) using the following equation:

$$\Delta A = \frac{\Delta A_{\infty}((1 + K_a[F] + [H]K_a) - \sqrt{(1 + K_a[F] + [H]K_a)^2 - 4K_a^2[F][H]})}{2K_a[H]}$$

where  $\Delta A = A - A_0$ ,  $[H]$  is the concentration of the host solution,  $[F]$  is the concentration of the fullerene,  $\Delta A_{\infty}$  is the absorbance difference at saturation of the binding sites, and  $K_a$  is the association constant. The parameters  $\Delta A_{\infty}$  and  $K_a$  are variable fitting parameters. The reported association constants are the average of the values calculated at 420 and 545 nm.

**Light Titration Experiments.** Solutions, typically in chlorobenzene, of either host **9** or a mixture of host **9** and  $C_{60}$  in quartz cuvettes (3 mL) were irradiated (1–3 min intervals) with a 500 W halogen lamp. The cuvette was placed about 15 cm in front of the lamp's glass window, and the UV–vis spectrum was measured periodically after each irradiation.

**4,10-Bis((triisopropylsilyl)ethynyl)-6,12-bis(benzo-1,3-dithiol-2-ylidene)dihydroanthanthrene (4).** A dry flask under nitrogen was charged with 4,10-bis((triisopropylsilyl)ethynyl)-6,12-bis(*gem*-dichlorovinylene)dihydroanthanthrene (**3**)<sup>9</sup> (100 mg, 0.125 mmol), 1,2-dithiobenzene (53 mg, 0.38 mmol), and 1,4-dioxane (4 mL) and was deaerated using a continuous flow of nitrogen for 5 min. Tetrabutylammonium hydroxide (1 M in MeOH, 0.75 mL, 0.75 mmol) was added in one portion, and the reaction was stirred at room temperature for 1 h. During that time, a purple precipitate formed. The reaction mixture was poured into MeOH (50 mL) and heated at reflux for 1 min. Once the mixture cooled to room temperature, the precipitate was recovered via filtration and afforded compound **4** as a purple solid (106 mg, 91%). <sup>1</sup>H NMR (500 MHz, CDCl<sub>3</sub>):  $\delta$  8.36–8.32 (m, 4H), 7.79–7.76 (m, 4H), 7.32–7.27 (m, 4H), 7.15–7.11 (m, 4H), 1.28–1.24 (m, 42H). <sup>13</sup>C NMR (125 MHz, CDCl<sub>3</sub>):  $\delta$  135.7, 134.7, 134.0, 133.7, 131.6, 130.1 (2C), 126.3, 126.1, 126.0 (2C), 125.9, 125.5, 125.0, 124.5, 122.5, 120.9, 120.1, 105.1, 97.4, 18.9, 11.5. HRMS (APPI+): *m/z* calcd for C<sub>58</sub>H<sub>59</sub>S<sub>4</sub>Si<sub>2</sub> 939.3033, found 939.3042 (M + H)<sup>+</sup>.

**4,10-Bis(3-((*tert*-butyldimethylsilyloxy)phenyl)anthanthrone (5).** A dry flask under nitrogen was charged with (3-bromophenoxy)-*tert*-butyldimethylsilane<sup>35</sup> (928 mg, 3.23 mmol) and anhydrous THF (7 mL), and the flask was cooled at –78 °C using a dry ice/acetone bath followed by the dropwise addition of *n*-BuLi (2.5 M in hexanes, 1.36 mL, 3.39 mmol). After 10 min, tributyltin chloride (1.10 g, 0.92 mL, 3.39 mmol) was added in one portion, and the reaction mixture was gradually warmed at 0 °C over 5 h. A separate flask was charged with 4,10-dibromoanthanthrone (500 mg, 1.07 mmol), dichlorobis(triphenylphosphine)palladium(II) (38 mg, 0.054 mmol), and *o*-dichlorobenzene (20 mL) and deaerated using a continuous flow of nitrogen for 10 min. The in situ prepared stannyl solution was transferred via syringe to the second reaction flask and heated at 105 °C overnight. Once cooled, the reaction mixture was poured into MeOH (100 mL), and the precipitate was recovered via filtration. The residue was washed with hot CHCl<sub>3</sub> to recover the crude product. The solvent was evaporated under reduced pressure, and the crude product was recrystallized from AcOEt (20–30 mL) to afford compound **5** as a red powder (670 mg, 80%). <sup>1</sup>H NMR (500 MHz, CDCl<sub>3</sub>):  $\delta$  8.60–8.56 (m, 2H), 8.35–8.28 (m, 4H), 7.77–7.70 (m, 2H), 7.48–7.41 (m, 2H), 7.24–7.18 (m, 2H), 7.11 (s, 2H), 7.04–7.00 (m, 2H), 1.04 (s, 18H), 0.29 (s, 12H). <sup>13</sup>C NMR (125 MHz, CDCl<sub>3</sub>):  $\delta$  182.9, 155.7, 142.8, 140.5, 134.0, 132.9, 130.6, 129.6, 129.2 (2C), 128.7, 127.8, 127.0, 124.6, 123.4, 122.1, 119.9, 25.7, 18.6, –4.3. HRMS (APPI+): *m/z* calcd for C<sub>46</sub>H<sub>47</sub>O<sub>4</sub>Si<sub>2</sub> 719.3007, found 719.3061 (M + H)<sup>+</sup>.

**4,10-Bis(3-((*tert*-butyldimethylsilyloxy)phenyl)-6,12-bis(*gem*-dichlorovinylene)dihydroanthanthrene (6).** A dry microwave flask under nitrogen was charged with compound **5** (400 mg, 0.55 mmol), triphenylphosphine (1.16 g, 4.45 mmol), and carbon tetrachloride (8.56 g, 5.4 mL, 55 mmol). The mixture was deaerated using a continuous flow of nitrogen for 10 min and gradually heated in a microwave apparatus at 150 °C over a period of 10 min, followed by

an additional 10 min at that same temperature. Once cooled, CH<sub>2</sub>Cl<sub>2</sub> was added, and the crude reaction mixture was filtered on silica gel and eluted with a CH<sub>2</sub>Cl<sub>2</sub>/hexanes (1:1) mixture to afford compound **6** as an orange powder (460 mg, 97%). <sup>1</sup>H NMR (500 MHz, CDCl<sub>3</sub>):  $\delta$  8.33–8.31 (m, 2H), 8.12 (s, 2H), 7.98–7.95 (m, 2H), 7.59–7.55 (m, 2H), 7.41–7.37 (m, 2H), 7.15–7.11 (m, 2H), 7.02 (s, 2H), 6.98–6.94 (m, 2H), 1.01 (s, 18H), 0.26 (s, 12H). <sup>13</sup>C NMR (125 MHz, CDCl<sub>3</sub>):  $\delta$  155.6, 141.4, 139.5, 132.54, 130.8, 130.3, 129.4, 128.6, 128.4, 127.6, 126.8, 126.4, 126.1, 125.7, 123.2, 121.9, 120.3, 119.5, 25.7, 18.3, –4.3. HRMS (APPI+): *m/z* calcd for C<sub>48</sub>H<sub>47</sub>C<sub>14</sub>O<sub>2</sub>Si<sub>2</sub> 851.1863, found 851.1871 (M + H)<sup>+</sup>.

**4,10-Bis(3-hydroxyphenyl)-6,12-bis(benzo-1,3-dithiol-2-ylidene)dihydroanthanthrene (7).** A dry flask under nitrogen was charged with compound **6** (300 mg, 0.352 mmol), benzene-1,2-dithiol (150 mg, 1.06 mmol), and 1,4-dioxane (12 mL) and deaerated using a continuous flow of nitrogen for 5 min. Tetrabutylammonium hydroxide (1 M in MeOH, 2.11 mL, 2.11 mmol) was added in one portion, and the reaction was stirred at room temperature for 1 h. Tetrabutylammonium fluoride (1 M in THF, 1.06 mL, 1.06 mmol) was added to cleave the remaining –O(TBS) groups. Aqueous NH<sub>4</sub>Cl was added to the reaction mixture, and it was extracted three times with a mixture of CHCl<sub>3</sub> and AcOEt, dried over Na<sub>2</sub>SO<sub>4</sub>, and evaporated under reduced pressure. The residue was purified by silica gel column chromatography (MeOH/CHCl<sub>3</sub>, 5:95, v/v) and recrystallized from CHCl<sub>3</sub> to afford compound **7** as a dark red solid (235 mg, 88%). <sup>1</sup>H NMR (500 MHz, DMSO-*d*<sub>6</sub>):  $\delta$  9.72 (s, 2H), 7.94 (s, 2H), 7.86 (d, *J* = 7.2 Hz, 2H), 7.71–7.65 (m, 4H), 7.51–7.43 (m, 4H), 7.36 (t, *J* = 7.7 Hz, 2H), 7.18–7.13 (m, 4H), 7.05–7.01 (m, 2H), 6.94–6.90 (m, 4H). <sup>13</sup>C NMR (125 MHz, DMSO-*d*<sub>6</sub>):  $\delta$  157.9, 141.3, 139.2, 135.3, 134.2, 133.5, 133.4, 130.3, 129.6, 129.4, 128.9 (3C), 126.3 (2C) 126.0, 125.8, 124.4, 123.7, 122.6, 121.8, 121.1, 117.3, 115.3. HRMS (APPI+): *m/z* calcd for C<sub>48</sub>H<sub>27</sub>O<sub>2</sub>S<sub>4</sub> 763.088, found 763.0880 (M + H)<sup>+</sup>.

**4,10-Bis(3-((6-bromohexyl)oxy)phenyl)-6,12-bis(benzo-1,3-dithiol-2-ylidene)dihydroanthanthrene (8).** A dry flask under nitrogen was charged with compound **7** (100 mg, 0.131 mmol) and dimethyl sulfoxide (4 mL). Tetrabutylammonium hydroxide (1 M in MeOH, 0.288 mL, 0.288 mmol) was added in one portion, and the reaction mixture was stirred for 10 min followed by the addition of 1,6-dibromohexane (0.639 g, 0.405 mL, 2.62 mmol) in one portion. After 4 h, the reaction mixture was poured into MeOH (100 mL) and filtered. The residue was purified by silica gel column chromatography (CHCl<sub>3</sub>/hexanes, 65:35, v/v) to afford compound **8** as a dark red solid (76 mg, 53%). <sup>1</sup>H NMR (500 MHz, CDCl<sub>3</sub>):  $\delta$  8.09 (s, 2H), 7.96–7.92 (m, 2H), 7.76–7.73 (m, 2H), 7.65–7.61 (m, 2H), 7.48–7.43 (m, 2H), 7.26–7.19 (m, 8H), 7.09–7.05 (m, 4H), 7.02 (dd, *J* = 4.2 Hz, *J* = 2.1 Hz, 2H), 4.05 (t, *J* = 6.3 Hz, 4H), 3.43 (t, *J* = 6.9 Hz, 4H), 1.94–1.83 (m, 8H), 1.57–1.51 (m, 8H). <sup>13</sup>C NMR (125 MHz, CDCl<sub>3</sub>):  $\delta$  159.0, 142.0, 138.9, 135.0, 134.6, 134.1, 133.9, 129.9, 129.8, 129.5, 126.4, 126.3, 126.0, 125.9, 125.5, 125.2, 124.5, 124.4, 123.6, 122.7, 120.9, 120.8, 116.4, 113.6, 67.8, 33.9, 32.7, 29.2, 28.0, 25.4. HRMS (APPI+): *m/z* calcd for C<sub>60</sub>H<sub>49</sub>Br<sub>2</sub>O<sub>2</sub>S<sub>4</sub> 1089.0957, found 1089.0961 (M + H)<sup>+</sup>.

**Host 9.** A dry flask under nitrogen was charged with compound **7** (46 mg, 0.060 mmol) and DMSO (4 mL). Tetrabutylammonium hydroxide (1 M in MeOH, 0.121 mL, 0.121 mmol) was added in one portion, and after 10 min, the reaction mixture was transferred via syringe to a second dry flask under nitrogen containing compound **8** (66 mg, 0.060 mmol) dissolved in DMSO (16 mL). After 2 h, an additional portion of tetrabutylammonium hydroxide (1 M in MeOH, 0.060 mL, 0.060 mmol) was added, and the resulting mixture was stirred for 2 h. The reaction mixture was poured into MeOH (100 mL) and filtered. The residue was purified by silica gel column

chromatography (CHCl<sub>3</sub>/hexanes, 80:20, v/v) and recrystallized twice from CHCl<sub>3</sub> to afford host **9** as a red/purple solid (28 mg, 27%).

The <sup>1</sup>H NMR spectrum of host **9** is complexified by the presence of conformational isomers. The product is analytically pure on TLC, and the HRMS and MALDI-TOF (Figure S8 in the Supporting Information) spectra confirmed its structure.

<sup>1</sup>H NMR (500 MHz, CDCl<sub>3</sub>, 50 °C): δ 8.09–8.03 (m, 1H), 7.95 (s, 2H), 7.92–7.80 (m, 4H), 7.76–7.67 (m, 1H), 7.61–7.50 (m, 4H), 7.46–7.35 (m, 6H), 7.22–7.10 (m, 14H), 7.10–6.88 (m, 16H), 4.10 (t, *J* = 6.1 Hz, 8H), 1.90 (t, *J* = 5.9 Hz, 8H), 1.67–1.61 (m, 8H). Acquisition of a <sup>13</sup>C NMR spectrum proved unsuccessful because of the compound's poor solubility. HRMS (APPI+): *m/z* calcd for C<sub>108</sub>H<sub>73</sub>O<sub>4</sub>S<sub>8</sub> 1690.3303, found 1690.3309 (M + H)<sup>+</sup>.

**Preparative Photooxidation Reaction: 4,10-Bis((triisopropylsilyl)ethynyl)anthanthrone (1) and 4,10-Bis((triisopropylsilyl)ethynyl)-6-(benzo-1,3-dithiol-2-ylidene)-12-oxodihydroanthanthrone (10).** In a cylindrical glass vessel equipped with a water-cooled borosilicate glass immersion well in which was enclosed a 450 W medium-pressure mercury lamp, compound **4** (30 mg, 0.032 mmol) and C<sub>60</sub> (11 mg, 0.015 mmol) were dissolved in benzene (ca. 500 mL). Compressed air was continuously bubbled through the solution using a long needle during the course of the irradiation. TLC analysis showed complete conversion of the starting material within 20 min of irradiation. The benzene solution was evaporated under reduced pressure, and the residue was purified using silica gel column chromatography (from CHCl<sub>3</sub>/hexanes, 20:80, v/v, to pure CHCl<sub>3</sub>) to afford compound **10** (7 mg, 25%) as a dark blue solid and crude compound **1** (contaminated with presumably benzo-1,3-dithiol-2-one), which was recrystallized from acetone to afford pure compound **1** (16 mg, 75%) as an orange solid. The <sup>1</sup>H NMR and HRMS data for **1** are consistent with the reported data.<sup>9</sup>

**Data for 10.** <sup>1</sup>H NMR (500 MHz, CDCl<sub>3</sub>): δ 8.91–8.87 (m, 1H), 8.81–8.87 (m, 1H), 8.70 (s, 1H), 8.51 (s, 1H), 8.44–8.40 (m, 1H), 7.97–7.89 (m, 3H), 7.38–7.32 (m, 2H), 7.21–7.16 (m, 2H), 1.33–1.16 (m, 42H). Due to limited solubility, the aliphatic region (δ 1.4–0.8) is contaminated with grease. Acquisition of a <sup>13</sup>C NMR spectrum proved unsuccessful because of the compound's poor solubility. HRMS (APPI+): *m/z* calcd for C<sub>51</sub>H<sub>55</sub>OS<sub>2</sub>Si<sub>2</sub> 803.3227, found 803.3243 (M + H)<sup>+</sup>.

## ■ ASSOCIATED CONTENT

### ● Supporting Information

<sup>1</sup>H and <sup>13</sup>C NMR spectra, structural comparison for compound **4**, UV–vis titration and stability control experiments and MALDI-TOF spectra for host **9**, and DFT-calculated coordinates and total energy for **4**. The Supporting Information is available free of charge on the ACS Publications website at DOI: 10.1021/acs.joc.5b00930.

## ■ AUTHOR INFORMATION

### Corresponding Author

\*E-mail: Jean-Francois.Morin@chm.ulaval.ca.

### Notes

The authors declare no competing financial interest.

## ■ ACKNOWLEDGMENTS

This work was supported by the Natural Sciences and Engineering Research Council of Canada (NSERC) through a Discovery Grant. We thank Quentin Verolet for his help in synthesis and Maude Desroches for MALDI-TOF analysis. J.-B.G. thanks the NSERC for a Ph.D. scholarship. We thank Heubach GmbH for providing 4,10-dibromoanthanthrone.

## ■ REFERENCES

- (1) Wudl, F.; Smith, G. M.; Hufnagel, E. J. *J. Chem. Soc. D: Chem. Commun.* **1970**, 1453–1454.
- (2) Martin, N. *Chem. Commun.* **2013**, 49, 7025–7027.

(3) Bechgaard, K.; Jacobsen, C. S.; Mortensen, K.; Pedersen, H. J.; Thorup, N. *Solid State Commun.* **1980**, 33, 1119–1125.

(4) (a) Bendikov, M.; Wudl, F.; Perepichka, D. F. *Chem. Rev.* **2004**, 104, 4891–4946. (b) Parker, C. R.; Leary, E.; Frisenda, R.; Wei, Z.; Jennum, K. S.; Glibstrup, E.; Abrahamsen, P. B.; Santella, M.; Christensen, M. A.; Della Pia, E. A.; Li, T.; Gonzalez, M. T.; Jiang, X.; Morsing, T. J.; Rubio-Bollinger, G.; Laursen, B. W.; Nørgaard, K.; van der Zant, H.; Agrait, N.; Nielsen, M. B. *J. Am. Chem. Soc.* **2014**, 136, 16497–16507.

(5) (a) Gao, X.; Qiu, W.; Liu, Y.; Yu, G.; Zhu, D. *Pure Appl. Chem.* **2008**, 80, 2405–2423. (b) Christensen, C. A.; Bryce, M. R.; Batsanov, A. S.; Becher, J. *Org. Biomol. Chem.* **2003**, 1, 511–522. (c) Bergkamp, J. J.; Decurtius, S.; Liu, S.-X. *Chem. Soc. Rev.* **2015**, 44, 863–874.

(6) (a) Perez, E. M.; Martin, N. *Chem. Soc. Rev.* **2008**, 37, 1512–1519. (b) Jeppesen, J. O.; Nielsen, M. B.; Becher, J. *Chem. Rev.* **2004**, 104, 5115–5132.

(7) (a) Iden, H.; Fontaine, F.-G.; Morin, J.-F. *Org. Biomol. Chem.* **2014**, 12, 4117–4123. (b) Isla, H.; Gallego, M. a.; Pérez, E. M.; Viruela, R.; Ortí, E.; Martín, N. *J. Am. Chem. Soc.* **2010**, 132, 1772–1773. (c) Grimm, B.; Santos, J.; Illescas, B. M.; Muñoz, A.; Guldi, D. M.; Martín, N. *J. Am. Chem. Soc.* **2010**, 132, 17387–17389. (d) González, S.; Martín, N.; Guldi, D. M. *J. Org. Chem.* **2002**, 68, 779–791. (e) Chen, G.; Bouzan, S.; Zhao, Y. *Tetrahedron Lett.* **2010**, 51, 6552–6556.

(8) (a) Liang, S.; Chen, G.; Zhao, Y. *J. Mater. Chem. C* **2013**, 1, 5477–5490. (b) Liang, S.; Zhao, Y.; Adronov, A. *J. Am. Chem. Soc.* **2013**, 136, 970–977.

(9) Giguère, J.-B.; Verolet, Q.; Morin, J.-F. *Chem.—Eur. J.* **2013**, 19, 372–381.

(10) (a) Giguère, J.-B.; Boismenu-Lavoie, J.; Morin, J.-F. *J. Org. Chem.* **2014**, 79, 2404–2418. (b) Giguère, J.-B.; Morin, J.-F. *J. Org. Chem.* **2013**, 78, 12769–12778. (c) Giguère, J.-B.; Sariciftci, N. S.; Morin, J.-F. *J. Mater. Chem. C* **2015**, 3, 601–606. (d) Lafleur-Lambert, A.; Giguère, J.-B.; Morin, J.-F. *Polym. Chem.* **2015**, DOI: 10.1039/C5PY00603A.

(11) Bill, N. L.; Ishida, M.; Bähring, S.; Lim, J. M.; Lee, S.; Davis, C. M.; Lynch, V. M.; Nielsen, K. A.; Jeppesen, J. O.; Ohkubo, K.; Fukuzumi, S.; Kim, D.; Sessler, J. L. *J. Am. Chem. Soc.* **2013**, 135, 10852–10862.

(12) Ueno, Y.; Bahry, M.; Okawara, M. *Tetrahedron Lett.* **1977**, 18, 4607–4610.

(13) Bryce, M. R. *J. Chem. Soc., Perkin Trans. 1* **1985**, 1675–1679.

(14) (a) Roncali, J. *Macromol. Rapid Commun.* **2007**, 28, 1761–1775. (b) Zhang, L.; Fonari, A.; Zhang, Y.; Zhao, G.; Coropceanu, V.; Hu, W.; Parkin, S.; Brédas, J.-L.; Briseno, A. L. *Chem.—Eur. J.* **2013**, 19, 17907–17916.

(15) (a) Mulla, K.; Zhao, Y. *J. Mater. Chem. C* **2013**, 1, 5116–5127. (b) Jones, A. E.; Christensen, C. A.; Perepichka, D. F.; Batsanov, A. S.; Beeby, A.; Low, P. J.; Bryce, M. R.; Parker, A. W. *Chem.—Eur. J.* **2001**, 7, 973–978.

(16) Schukat, G.; Fanghänel, E. *Sulfur Rep.* **1996**, 18, 1–278.

(17) Moore, A. J.; Bryce, M. R. *Synthesis* **1991**, 1991, 26–28.

(18) Christensen, C. A.; Batsanov, A. S.; Bryce, M. R. *J. Org. Chem.* **2007**, 72, 1301–1308.

(19) Kao, H.-L.; Lee, C.-F. *Org. Lett.* **2011**, 13, 5204–5207.

(20) Hurlley, W. R. H.; Smiles, S. *J. Chem. Soc.* **1926**, 129, 2263–2270.

(21) (a) Bajwa, G. S.; Berlin, K. D.; Pohl, H. A. *J. Org. Chem.* **1976**, 41, 145–148. (b) Gimbert, Y.; Moradpour, A.; Dive, G.; Dehareng, D.; Lahlil, K. *J. Org. Chem.* **1993**, 58, 4685–4690. (c) Mizuno, M.; Cava, M. P. *J. Org. Chem.* **1978**, 43, 416–418.

(22) Frisch, M. J.; Trucks, G. W.; Schlegel, H. B.; Scuseria, G. E.; Robb, M. A.; Cheeseman, J. R.; Scalmani, G.; Barone, V.; Mennucci, B.; Petersson, G. A.; Nakatsuji, H.; Caricato, M.; Li, X.; Hratchian, H. P.; Izmaylov, A. F.; Bloino, J.; Zheng, G.; Sonnenberg, J. L.; Hada, M.; Ehara, M.; Toyota, K.; Fukuda, R.; Hasegawa, J.; Ishida, M.; Nakajima, T.; Honda, Y.; Kitao, O.; Nakai, H.; Vreven, T.; Montgomery, J. A., Jr.; Peralta, J. E.; Ogliaro, F.; Bearpark, M. J.; Heyd, J.; Brothers, E. N.; Kudin, K. N.; Staroverov, V. N.; Kobayashi, R.; Normand, J.;



Raghavachari, K.; Rendell, A. P.; Burant, J. C.; Iyengar, S. S.; Tomasi, J.; Cossi, M.; Rega, N.; Millam, N. J.; Klene, M.; Knox, J. E.; Cross, J. B.; Bakken, V.; Adamo, C.; Jaramillo, J.; Gomperts, R.; Stratmann, R. E.; Yazyev, O.; Austin, A. J.; Cammi, R.; Pomelli, C.; Ochterski, J. W.; Martin, R. L.; Morokuma, K.; Zakrzewski, V. G.; Voth, G. A.; Salvador, P.; Dannenberg, J. J.; Dapprich, S.; Daniels, A. D.; Farkas, Ö.; Foresman, J. B.; Ortiz, J. V.; Cioslowski, J.; Fox, D. J. *Gaussian 09*; Gaussian, Inc.: Wallingford, CT, 2009.

(23) Batsanov, A. S.; Bryce, M. R.; Coffin, M. A.; Green, A.; Hester, R. E.; Howard, J. A. K.; Lednev, I. K.; Martín, N.; Moore, A. J.; Moore, J. N.; Ortí, E.; Sánchez, L.; Savirón, M.; Viruela, P. M.; Viruela, R.; Ye, T.-Q. *Chem.—Eur. J.* **1998**, *4*, 2580–2592.

(24) (a) Tashiro, K.; Aida, T. *Chem. Soc. Rev.* **2007**, *36*, 189–197. (b) Tashiro, K.; Aida, T.; Zheng, J.-Y.; Kinbara, K.; Saigo, K.; Sakamoto, S.; Yamaguchi, K. *J. Am. Chem. Soc.* **1999**, *121*, 9477–9478.

(25) Hasobe, T.; Oki, H.; Sandanayaka, A. S. D.; Murata, H. *Chem. Commun.* **2008**, 724–726.

(26) Giguère, J.-B.; Morin, J.-F. *Org. Biomol. Chem.* **2012**, *10*, 1047–1051.

(27) Connors, K. A. *Binding Constants: The Measurement of Molecular Complex Stability*; Wiley & Sons: New York, 1987.

(28) (a) Canevet, D.; Gallego, M.; Isla, H.; de Juan, A.; Pérez, E. M.; Martín, N. *J. Am. Chem. Soc.* **2011**, *133*, 3184–3190. (b) Pérez, E. M.; Sánchez, L.; Fernández, G.; Martín, N. *J. Am. Chem. Soc.* **2006**, *128*, 7172–7173.

(29) Possible C<sub>60</sub> contamination might artificially increase the yield.

(30) Mroz, P.; Tegos, G. P.; Gali, H.; Wharton, T.; Sarna, T.; Hamblin, M. R. *Photochem. Photobiol. Sci.* **2007**, *6*, 1139–1149.

(31) (a) Kyriakopoulos, J.; Papastavrou, A. T.; Panagiotou, G. D.; Tzirakis, M. D.; Triantafyllidis, K. S.; Alberti, M. N.; Bourikas, K.; Kordulis, C.; Orfanopoulos, M.; Lycourghiotis, A. *J. Mol. Catal. A: Chem.* **2014**, *381*, 9–15. (b) Vougioukalakis, G. C.; Angelis, Y.; Vakros, J.; Panagiotou, G.; Kordulis, C.; Lycourghiotis, A.; Orfanopoulos, M. *Synlett* **2004**, 971–974. (c) Tokuyama, H.; Nakamura, E. *J. Org. Chem.* **1994**, *59*, 1135–1138.

(32) Clennan, E. L.; Pace, A. *Tetrahedron* **2005**, *61*, 6665–6691.

(33) Sarhan, A. E.-W. A. O.; Murakami, M.; Izumi, T. *Monatsh. Chem.* **2002**, *133*, 1055–1066.

(34) (a) Clar, E. *The Aromatic Sextet*; Wiley: New York, 1972. (b) Solà, M. *Front. Chem.* **2013**, *1*, 22.

(35) Boße, F.; Tunoori, A. R.; Maier, M. E. *Tetrahedron* **1997**, *53*, 9159–9168.